Journal of Harbin Engineering University Vol 44 No. 5
ISSN: 1006-7043 May 2023

Finite Element Analysis of M40 PET Fiber Concrete

Nirav M. Patel[1], Dr. M. N. Patel[2]
[1]*Assistant Professor, Dept. of Civil Engineering, Parul Institute of Engineering and Technology, Parul University, Vadodara, Gujarat, India.*
[2]*Advisor, Parul University, Vadodara, Gujarat, India.*
[1]nirav.patel20968@paruluniversity.ac.in, [2]nmp1290@gmail.com

Abstract -By using PET waste fiber, the failure behavior of the beam-column junction may be minimized or up to some extend it may be avoided. With the variation of composition different seismic performance of the concrete joint could be adjusted. The FEM analysis in ABAQUS software, has been carried out to compare the behavior of conventional concrete and PET waste fiber reinforced concrete beam column joint under cyclic loading. Concrete mix has been designed to obtain a concrete grade of M40. Seven numbers of exterior beam column joints modeled to one fourth of a prototype of a building. The first joint was made with the conventional concrete and designed as per IS 1893 (part 1): 2002 and the reinforcement in the joint portion detailed as per the IS 13920: 2016, for the ductility requirement. The additional six specimen designed with the various inclusion of the PET waste fibers (0.25 % to 1.50 %) at the joint region. The beam-column joint having 0.50 % to 1.00 % inclusion of PET fibers have better performance in the strength, load carrying capacity, energy dissipation capacity, joint shear capacity and ductility behavior at the joint region. PET waste fiber inclusion in the concrete can provide the best solution for the waste management and it also reduce the cost of the reinforced concrete by 15 % to 20 % with better seismic performance.
Keywords *-Strength performance, PET waste fiber, Failure behavior, Exterior beam-column, Waste management.*

Introduction

The long-term performance of structures has become vital to the economics of all nations. Concrete has been the major material for giving reliable and stable infrastructure since the initiation of ancient communities. So many research works were been carried out in the 20th century [1]. As a result, new materials and composites have been developed and improved types of cement evolved. Nowadays, concrete structures having a compressive strength exceeding 140 MPa are being built all over the world [2]. In research laboratories, the compressive strength of concrete reaches as high as 800 MPa is being developed. Damage in reinforced concrete structures is mainly attributed to shear force due to the inadequate detailing of reinforcement and the lack of transverse steel and confinement of concrete in the structural elements [3]. High-strength concrete is brittle, demonstrating an inadequate capacity to dissipate and absorb inelastic energy. The beam-column joints that are subjected to reverse cyclic loading require great care in detailing. The acceptable interpretation of a beam-column joint, especially under seismic loads, depends highly on the lateral captivity of the joint. The behavior of beam-column joints by using various fiber reinforced concrete under vibrating conditions has been a major research area for many years [4]. The present study deals with the conventional reinforcement detailing in the beam-column joint and providing plastic waste fiber reinforced concrete. This fiber-reinforced concrete at the joint region has better compressive, flexural, and tensile strength compared to conventional concrete [5].

The plastic production is one of the fastest production units in the world. Plastic packaging substances are rejected as waste, after fulfilling their service. Plastics remain non-biodegradable for many years and create a great threat to the environment [6]. Though recycling waste plastic is a possible option to reduce the threat, it required higher energy and vast manpower. Since recycling waste plastic requires all together with different technology and vast resources. Using the waste plastic directly within the concrete industry's needs can be considered a novel approach. As concrete industries utilize conventional resources [7]. Different fibers such as steel, glass, carbon, nylon, etc. are showing good tensile strength their pre-processing overheads are more. On the contrary plastic fibers required straining which is far less expensive as compared to its peer fibers [8-10].

The beam-column joint region is a very important area in the seismic-resaistant frame; particularly for the external T-joints as they transfer greater shear forces compared with inner joints. During an earthquake, large lateral forces are applied on the side of the building and the shear forces caused by the longitudinal beam steel bar penetrate the joint core [11]. The shear force may occur in a corner-to-corner diagonal tension failure. Joints not designed to withstand high shear, such as pre-70's beam-column joints are likely to encounter

shear failure in joints. Well, confined joints give superior behavior, but the stirrups and hoops in the joint region may cause steel blockage [12-13]. Considering the benefits of plastic waste fiber reinforced concrete described earlier, such as high energy absorption capacity, improved tensile strength, and damage tolerance of concrete, using PET fibers in beam-column joints may be a constructive method for minimizing the stirrup congestion and enhancing the shear capacity of joints in seismic-resistance portal-frames [14-21].

Analytical Program Using ABAQUS

2.1.Details of Test Specimen and Reinforcement

The test specimen joint design includes beam and column with 90 mm X 110 mm and 90 mm X 90 mm respectively. At the joint, beam longitudinal reinforcement at the top was 1.52 % and at the bottom was 1.00 % of gross area. The vertical longitudinal reinforcement of the joint is 2.40 %. The amount of reinforcement of hoops and shear at the joint portion was 2.25 % for the seismic region and another portion i.e., for the nominal zone was 1.10 % considered. Figures 1a and 1b show seismic joint and ordinary & fibrous joint respectively. For a seismic joint, this hoop spacing is 20 mm for a distance of 180 mm ($2*d_b$) (d_b = effective depth of beam) from the face of the column in the beam and at a distance of 90 mm (d_b) from the bottom and top of the beam in the column. The fibrous joints were cast by using fiber reinforced concrete in the joint region for a distance of two times effective depth from the face of the column on beam and one time the effective depth from the face of the beam on either side of the column. The effective cover for main reinforcement is 20 mm.

2.2.Analysis Using FE Software

2.2.1. Part

Part Module used to create the geometry of the part. Figure 2 shows concrete is modelled as a 3D deformable solid extrusion type element and reinforcement is defined as a 3D deformable wire planer type of element.

2.2.2. Properties

Users can specify the properties of a part or part region by creating a section and assigning it to the part using the property module. ABAQUS software provides different models for simulating the damage like, Concrete damaged plasticity, Smeared crack model etc. Material property for concrete, steel, and PET fiber is explained in the above material property section.

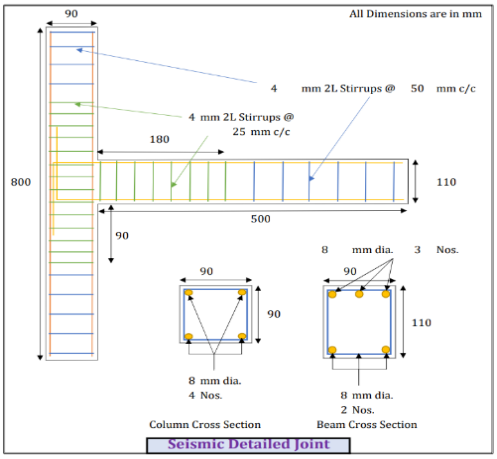

Fig. 1aSeismic Detailed Joint

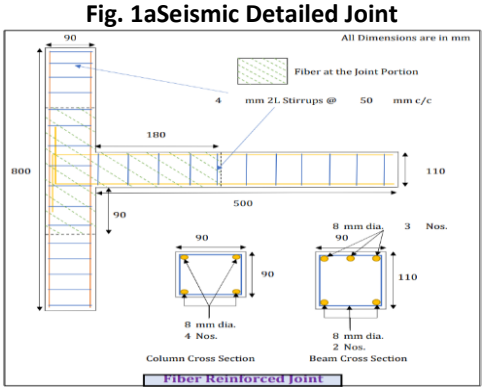

Fig. 1bFiber Reinforced Joint

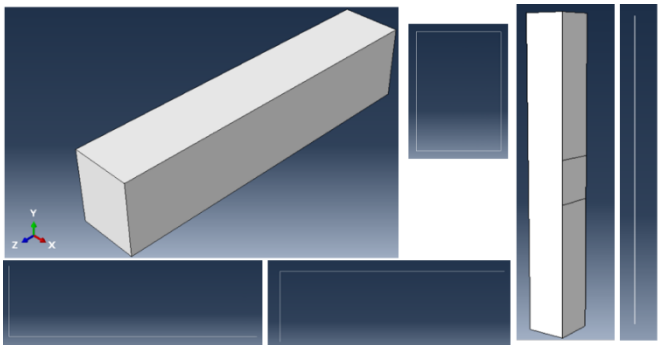

Fig. 2 Modelling of Concrete and Reinforcement part

2.2.3. Assembly

This is used to assemble the model and create an assembly. Each part that was created previously is oriented to create assembly by different tools like translate, rotate, linear pattern etc. The Assembly of the beam-column joint section is shown in Figure 3.

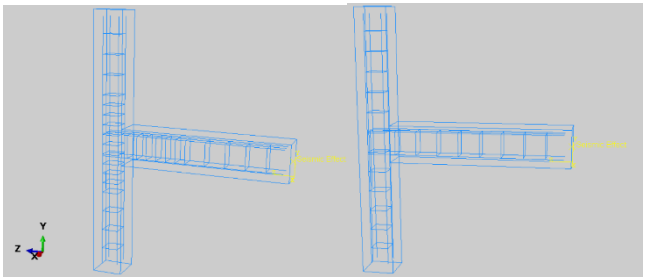

Fig. 3Assembly of reinforcement and RC beam

2.2.4. Dynamic Explicit Step

For highly non-linear quasi-static problem can be solved as a dynamic problem with slow load increment to generate negligible inertial forces. Dynamic explicit integration scheme can be used for its advantages of convergence problem, low resource consumption, better suitability for post-failure analysis.

2.2.5. Tie Constraint

For defining interaction between beam and column, the perfect bond is assumed between them. In perfect bonding, there is no translation allowed between beam and column. Tie constraint is used for the perfect bond. In the tie, the constraint beam is selected as the master surface and the column is considered as slave surface as shown in figure 4.

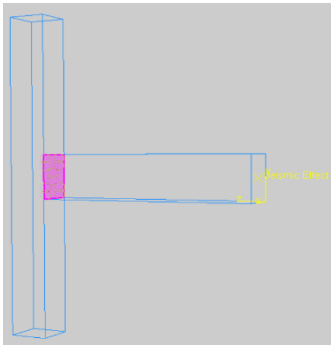

Fig. 4Tie constraint between column and beam

2.2.6. Embedded Region

Embedded region constraint is used for defining that elements or groups of elements are embedded in the host element. For defining interaction between reinforcement and concrete, an embedded constraint is used. Reinforcement is selected as embedded region and concrete is selected as the host element. Figure 5 embedded connectivity between reinforcement and concrete.

2.2.7. Coupling Constraint

The coupling constraint in ABAQUS provides coupling between a reference node and a group of nodes referred to as the coupling nodes. Coupling constraint is used to provide seismic loading about the longitudinal axis. The reference point is selected as a control point and the side surface of the beam is selected as surface as shown in figure 6.

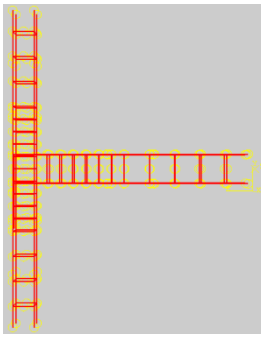

Fig. 5Embedded connectivity between reinforcement and concrete

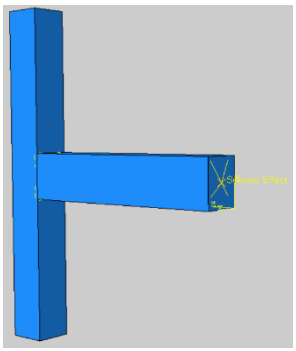

Fig. 6Coupling constraint for the seismic loading

2.2.8. Load and Boundary Condition

The boundary condition is provided in the predefined initial step. Fixed support is provided at both ends of the column. Loading is applied in terms of displacement in the user-created step. Figure 7 indicates that the seismic load is applied in direction of the longitudinal axis of the beam at the reference point created on the free end of the beam.

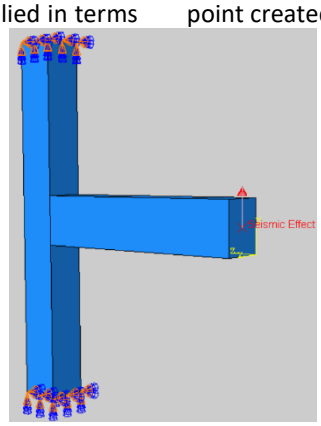

Fig. 7Loading and boundary condition

2.2.9. Mesh

Concrete has meshed with C3D8R: A 8-node linear brick element with 3D stress element family. Solid elements have only three translation degrees of the free dome at every 8 nodes.

Reinforcement has meshed with T3D2: A 2 node truss element. Truss elements have only axial forces no moment and perpendicular forces are supported. The cross-sectional area of the reinforcement bar has to be specified to truss elements otherwise unit area was assumed by ABAQUS by defaults.

Materials and Methods

3.1.Concrete

Concrete is defined as an isotropic material before yielding. But after yielding cracking model is defined for nonlinear analysis. In the isotropic elasticity option modulus of elasticity, poison's ratio and density of concrete are defined. Poisson's ratio for concrete is assumed as 0.2. Modulus of elasticity is defined according to IS 456 as shown in the below Equation 1 [22-23].

$$E = 5000 \times \sqrt{f_{ck}} \quad (1)$$

To predict the non-linear behavior of concrete damaged plasticity model is used. The concrete damaged plasticity model uses stress v/s strain relationships to correlate parameters for relative concrete damage for both tension and compression. In addition to these basic parameters that identify stress-strain relationships, parameters based upon

the microstructure of concrete must also be identified. These parameters are as shown in Table 1 [24].

Table 1. Concrete parameter

Dilation Angle	Eccentricity	f_{bo}/f_{co}	K	Viscosity Parameter
36	0.1	1.16	0.667	0

3.1.1. Compressive Behavior

The stress-strain relationship proposed by Kent and park model was used for the uniaxial compressive stress-strain curve as:

$$\sigma_c = (1 - d_c)E_0\ (\varepsilon_c - \varepsilon_c^{pl,h}) \quad (2)$$

$$\varepsilon_c^{in,h} = \varepsilon_c - \frac{\sigma_c}{E_0} \quad (3)$$

$$\varepsilon_c^{pl,h} = \varepsilon_c - \frac{\sigma_c}{E_0}\left(\frac{1}{1-d_c}\right) \quad (4)$$

$$\varepsilon_c^{pl,h} = \varepsilon_c^{in,h} - \frac{d_c}{(1-d_c)}\frac{\sigma_c}{E_0} \quad (5)$$

$$\sigma_c = \sigma_{cu}\left[2\left(\frac{\varepsilon_c}{\varepsilon'_c}\right) - \left(\frac{\varepsilon_c}{\varepsilon'_c}\right)^2\right] \quad (6)$$

$$d_c = 1 - \frac{\sigma_c}{\sigma_{cu}} \quad (7)$$

σ_c = Yield Stress

σ_{cu} = Ultimate Yield Stress

ε_c = Strain

$\varepsilon_c^{in,h}$ = Inelastic Strain

$\varepsilon_c^{pl,h}$ = Plastic Strain

d_c = Damage Parameter

3.1.1. Tension Behavior

Linear behavior is defined up to cracking of concrete and after that tension stiffening part is defined linearly decreasing and becoming zero at strain value 0.01.

$$\sigma_t = (1 - d_t)E_0\ (\varepsilon_t - \varepsilon_t^{pl,h}) \quad (8)$$

$$\varepsilon_t^{ck,h} = \varepsilon_t - \frac{\sigma_t}{E_0} \quad (9)$$

$$\varepsilon_t^{pl,h} = \varepsilon_t - \frac{\sigma_t}{E_0}\left(\frac{1}{1-d_t}\right) \quad (10)$$

$$\varepsilon_t^{pl,h} = \varepsilon_t^{ck,h} - \frac{d_t}{(1-d_t)}\frac{\sigma_t}{E_0} \quad (11)$$

$$d_t = 1 - \frac{\sigma_t}{\sigma_{t0}} \quad (12)$$

σ_t = Tensile Stress

ε_t = Strain

$\varepsilon_t^{ck,h}$ = Cracking Strain

$\varepsilon_t^{pl,h}$ = Plastic Strain

d_t = Damage Parameter

No softening effect is considered for numerical simulation. Figure 8 shows the stress-strain graph of concrete under compression & tension. Tables 2 & 3 show values of stress, strain and compression damage parameters data for M40 grade concrete under compression & tension respectively.

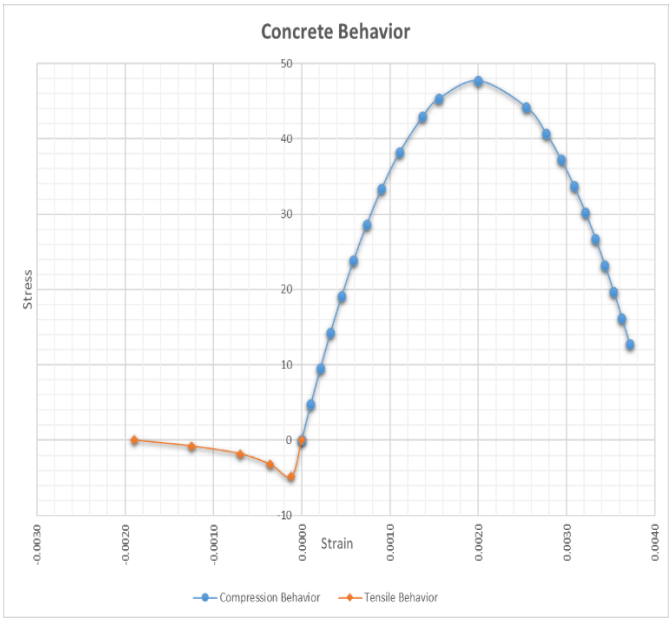

Fig. 8Loading and boundary condition

Table 2. Stress-strain for M40 grade concrete under compression

Yield Stress	Strain	Inelastic Strain	Damage Parameter	Inelastic Strain
σ_c	ε_c	ε_c^{in}	d_c	ε_c^{in}

23.86	0.000586	0.000000	0	0.000000
28.64	0.000735	0.000032	0	0.000032
33.41	0.000905	0.000084	0	0.000084
38.18	0.001106	0.000168	0	0.000168
42.95	0.001368	0.000313	0	0.000313
45.34	0.001553	0.000440	0	0.000440
47.73	0.002000	0.000828	0	0.000828
44.23	0.002542	0.001456	0.07	0.001456
40.73	0.002766	0.001766	0.15	0.001766
37.23	0.002938	0.002024	0.22	0.002024
33.73	0.003083	0.002255	0.29	0.002255
30.23	0.003211	0.002469	0.37	0.002469
26.73	0.003327	0.002671	0.44	0.002671
23.23	0.003433	0.002863	0.51	0.002863
19.73	0.003532	0.003048	0.59	0.003048
16.23	0.003625	0.003226	0.66	0.003226
12.73	0.003713	0.003400	0.73	0.003400

Table 3. Stress-strain for M25 grade concrete under tension

Tensile Stress	Strain	Cracking Strain	Damage Parameter	Cracking Strain
f_{ct}	ε_{ct}	ε_t^{ck}	d_t	ε_t^{ck}
4.1649	0.000138	0	0	0
2.7766	0.000414	0.000322	0.333333	0.000322
1.5618	0.000810	0.000758	0.625000	0.000758
0.6941	0.001447	0.001424	0.833333	0.001424
0.0000	0.002205	0.002205	1.000000	0.002205

3.2.Reinforcement

Parameter for material modelling up to elastic limit include young's modulus of elasticity which is equal to 200000 N/mm^2 and poison's ratio for steel equal to 0.3. Plastic behavior is defined as the stress v/s plastic strain relationship. The Stress-Strain curve for Reinforcement bars embedded in reinforcement is proposed by Belarbi and Hsu is used [25]. Figure 9 shows the stress-strain relationship of FE–500 reinforcement.

3.3.PET plastic waste fiber

The PETs were cut from the scrape water and soda bottles into fiber form with the help of a shredding machine, as shown in Figure 10. The investigation was carried out with a constant length and width of 20 mm and 2.5 mm fibers respectively. The General and test properties of PET are listed in Table 4. The fibers were added to the concrete in varying fractions, ranging from 0% to 1.5%, with a constant interval of 0.25 by mix volume.

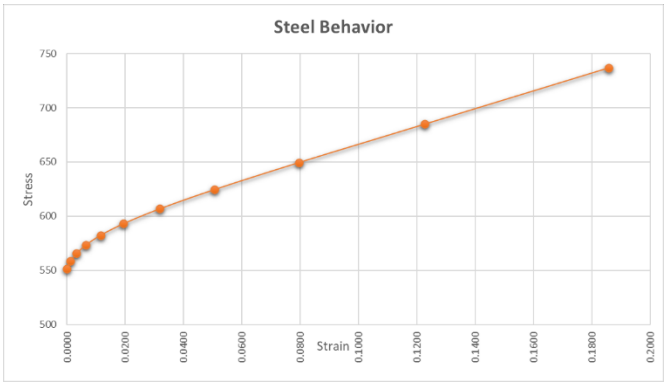

Fig. 9Stress-strain relationship of FE-500 steel reinforcement

Fig. 10Shredded PET waste fibers

Table 4. Properties of PET

Sr. No	Properties	Unit	Value
1	Length	mm	25
2	Width	mm	2 – 3
3	Thickness	mm	0.0625
4	Aspect Ratio	-	400
5	Specific Gravity	-	1.39
6	Tensile Strength	N/mm^2	137.30
7	Elongation	%	64.00

Results and Discussion

4.1. Load Deflection Behaviour

From the belowfigure 11 and Table 5, it is observed that the specimen M40_P_0.75 which was cast by using M40 concrete had maximum ultimate load compared to all other specimens. It is 24.17 % greater than the specimen cast by using ordinary M40 concrete with seismic detail. Specimen M40_P_1.50 had minimum ultimate load having 32.83 % lowest than the other specimen.

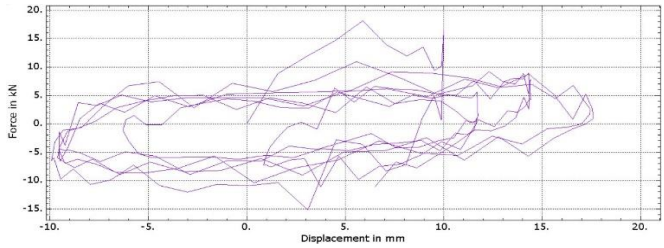

Fig. 11a Load Deflection curve for Specimen M40_S

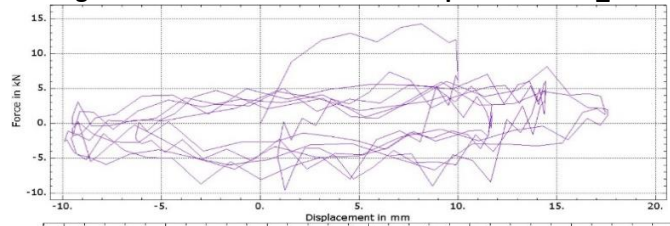

Fig. 11b Load Deflection curve for Specimen M40_P_0.25

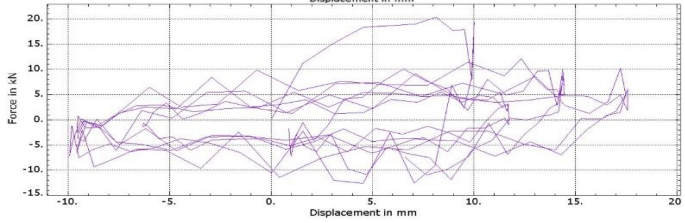

Fig. 11c Load Deflection curve for Specimen M40_P_0.50

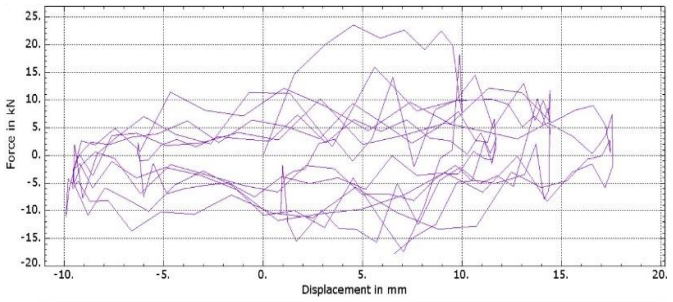

Fig. 11d Load Deflection curve for Specimen M40_P_0.75

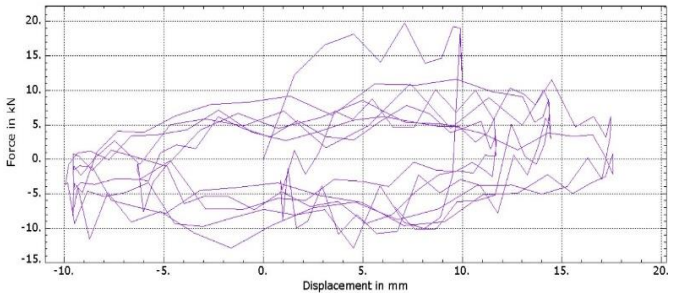

Fig. 11e Load Deflection curve for Specimen M40_P_1.00

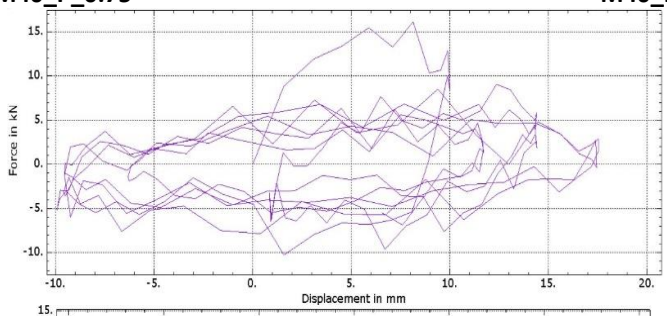

Fig. 11f Load Deflection curve for Specimen M40_P_1.25

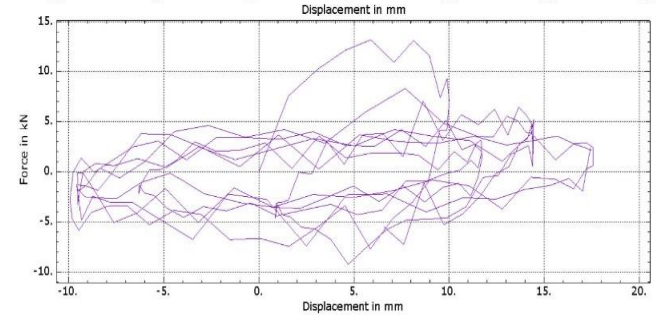

Fig. 11g Load Deflection curve for Specimen M40_P_1.50

Fig. 11 Load Deflection curve for different M40 Specimens

Table 5. Ultimate Load and Deflection of M40 Concrete

Sr. No.	Specimen ID	Ultimate Load (P_u) kN		Ultimate Deflection (δ) mm	
		Upward	Downward	Upward	Downward
1	M40_S	18.153	15.181	17.576	9.917
2	M40_P_0.25	14.320	9.646	17.567	9.919
3	M40_P_0.50	20.313	15.097	17.565	9.927
4	M40_P_0.75	23.559	17.832	17.569	9.919
5	M40_P_1.00	19.794	14.821	17.559	9.938
6	M40_P_1.25	16.120	12.313	17.553	9.935
7	M40_P_1.50	13.177	9.213	17.577	9.920

4.2. Load Carrying Capacity

The results show that the upward and download load carrying capacity of the PET fiber concrete increase up to 0.75 % of the increment of the fiber dosage after that again it indicates the down fall in the load carrying capacity. by keeping deflection amount constant, loading values are identified. Load carrying capacity of all the variations are shown in the Table 6. 0.75 % inclusion of waste PET fiber in the M40 grade of concrete gives up to 24 % higher load carrying capacity compare to conventional concrete at constant deflection. Figure 12 indicates the load carrying capacity and its % variation for the all the analysis.

Table 6. Load carrying capacity of M40 Concrete

Parameters	Units	M40_S	M40_0.25%	M40_0.50%	M40_0.75%	M40_1.00%	M40_1.25%	M40_1.50%
Ultimate Upward Load	kN	18.1534	14.3200	20.3128	23.5594	19.7939	16.1201	13.1769
Ultimate Downward Load	kN	15.1810	9.6456	15.0967	17.8316	14.8206	12.3131	9.2126
Total Load	kN	33.3344	23.9656	35.4095	41.3910	34.6145	28.4332	22.3895
Ultimate Upward Deflection	mm	17.5755	17.5674	17.5650	17.5693	17.5583	17.5527	17.5769
Ultimate Downward Deflection	mm	9.9174	9.9194	9.9269	9.9195	9.9376	9.9350	9.9198
Total Deflection	mm	29.4320	27.4868	27.4919	27.4888	27.4959	27.4877	27.4967

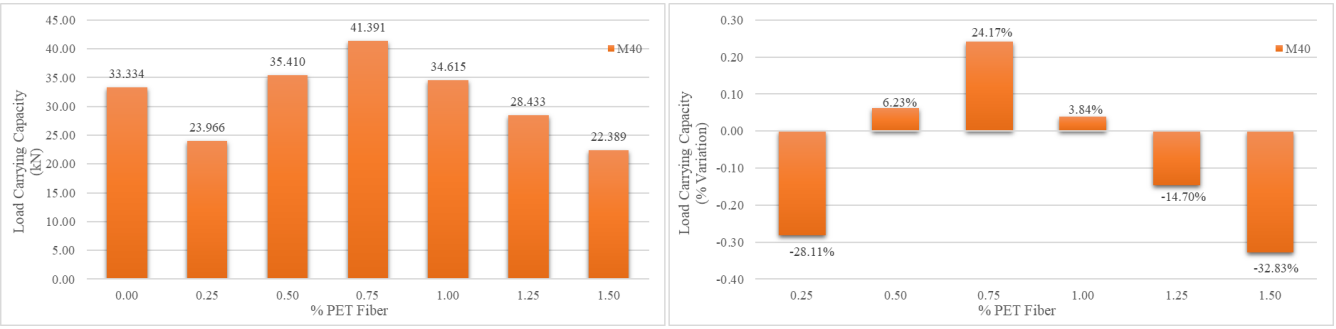

Fig. 12 Load carrying capacity and its % variations

4.3. Energy Dissipation Capacity

The area enclosed by a hysteresis loop at given cycle represents the energy dissipated by the specimen during the cycle. The Figure 13 shows the energy dissipating capacity of all the specimens. From the figure it is observed that compared to ordinary specimen the energy dissipation capacity is improved by 36.80 % by the addition of 0.75 % of PET waste fiber.

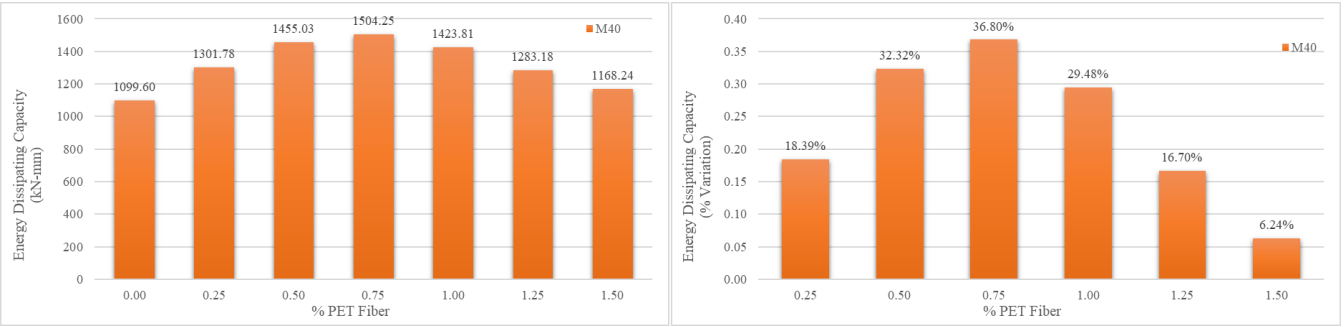

Fig. 13 Energy dissipating capacity of all the specimens

4.4. Ultimate Stress

From the Figures 14 and15, it is observed that the ultimate stiffness of the fiber mix concrete reaches optimum value for 0.75% for M40 with compare to basic concrete mix. M40 concrete mix indicated maximum increment of 6.83% at 0.75% dosage of fibres.

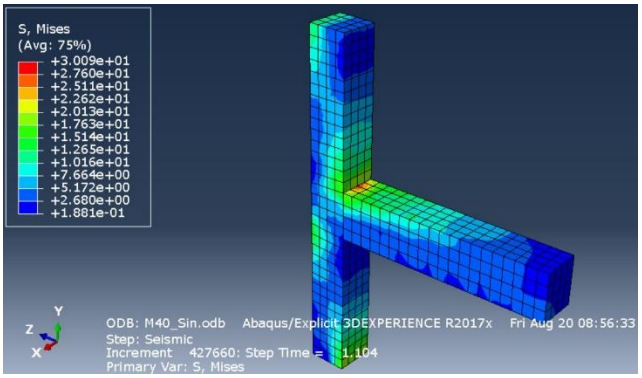

Fig. 14aUltimate Stress M40_S

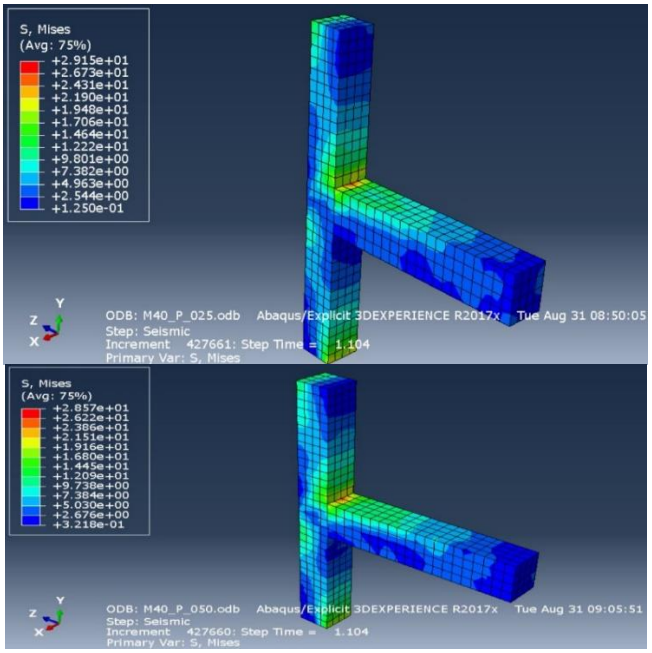

Fig. 14bUltimate Stress M40_P_0.25

Fig. 14c Ultimate Stress M40_P_0.50

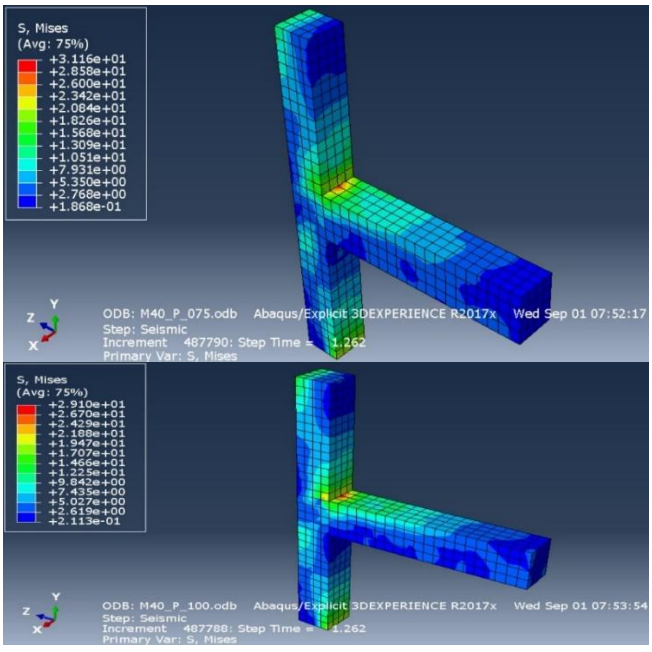

Fig. 14dUltimate Stress M40_P_0.75

Fig. 14eUltimate Stress M40_P_1.00

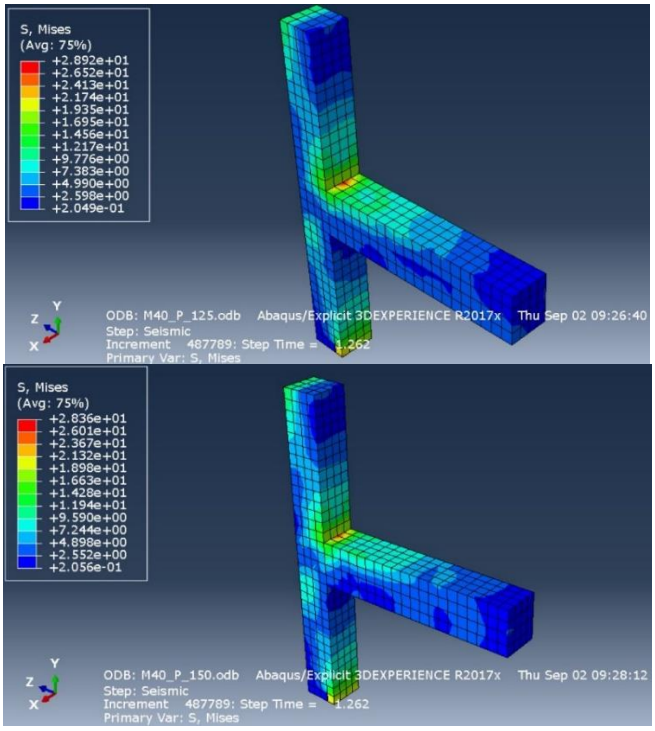

Fig. 14fUltimate Stress M40_P_1.25 **Fig. 14gUltimate Stress M40_P_1.50**

Fig. 14 Ultimate Stress of all specimens

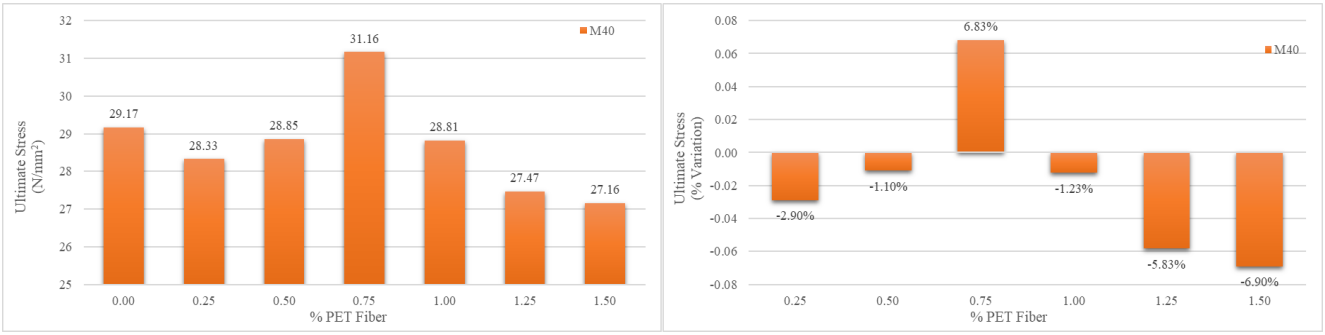

Fig. 15 Ultimate Stress comparison of all specimens

4.5. Joint Shear

For the exterior beam-column joint the horizontal and vertical joint shear stresses (τ_{jh}, τ_{jv}) can be calculated using the following formula [26].

$$\tau_{jh} = \frac{P_u}{A^h core}\left[\frac{L_b}{d_b} - \frac{L_b+0.5D_b}{L_c}\right] \quad (13)$$

$$\tau_{jv} = \frac{P_u}{A^v core}\left[1 - \left(\frac{L_b+0.5D_c}{L_c}\right)\left(\frac{L_c-D_b}{d_c}\right)\right] \quad (14)$$

Where, L_b and L_c are the length of beam and column respectively; D_b and Dc are the total depth of beam and column respectively; d_b and dc are the effective depth of beam and column respectively; A^hcore and A^vcore are the horizontal and vertical cross-sectional areas of the joint core resisting the horizontal and vertical joint shear forces,respectively. P_u is the ultimate load. Table 7 shows ultimate shear capacity of the joint using M40 Concrete. 0.75 % inclusion of PET waste fiber shows better result for both vertical and horizontal joint shear stress compare to all other variants.

Table 7. Ultimate shear capacity of the joint using M40 Concrete

Test Specimen	Joint Shear Stress	
	Horizontal	Vertical
M40_S	10.892	9.621
M40_0.25%	8.592	7.590
M40_0.50%	12.188	10.766
M40_0.75%	14.136	12.486

M40_1.00%	11.876	10.491
M40_1.25%	9.672	8.544
M40_1.50%	7.906	6.984

4.6. Curvature Ductility Factor

The capacity of the member to deform beyond its initial yield deformations with minimum loss of strength and stiffness depends upon the ductility factor which is defined as the ratio of the ultimate deformation to its yield deformation at first yield. Ductility may be defined easily in the case of elastoplastic behaviour [27]. Ductility factors in beam-column joint have been defined in terms curvature at critical section as;

$$Curvature\ ductility\ factor = \frac{\emptyset_u}{\emptyset_y} \quad (15)$$

$$\emptyset_u = Curvature\ at\ peak\ load = \frac{e_t + e_b}{(d_b + a)} \quad (16)$$

$$\emptyset_y = Curvature\ at\ yield\ = \frac{f_y}{E_s(d_b - x)} \quad (17)$$

$e_t = strainintopreinforcement$
$e_b = straininbottomreinforcement$
$a = compressivereinforcementcover$
$E_s = Modulusofelasticityofsteel$
$x = depthofneutralaxis$

Curvature ductility factor and its % variation for all the specimens are shown in figure 16. From the chart it may be indicated that the PET fiber reinforced specimen shows decrement in curvature ductility till 0.50 % inclusion and after that ductility factor increase by increasing the PET waste fiber.

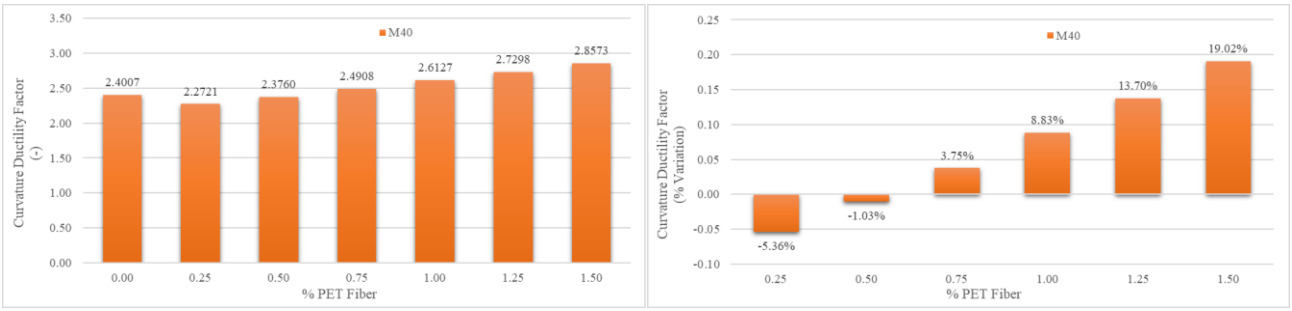

Fig. 16Curvature Ductility Factors for all specimen

4.7. Joint Distortion Factor

The stress conditions in the beam-column joint are indeed rather complicated. The interior core of the joint bounded by the longitudinal bars in the beam and column is in fact subjected to larger shear stresses and therefore has more distortion compared with the entire joint. The two LVDTs mounted diagonally on the rear face on the joint were used to measure the distortion of the interior core of the joint.

$$Joint\ Distorion = \left(\left(\frac{e_1 + e_2}{2}\right) \times \left(\frac{D_l}{h_j \times b_j}\right)\right) \quad (17)$$

$e_{1,}e_2$
$= Changesinlengthofthediagonaljointregioninmm$
$D_l =$ Initial diagonal length in mm
$h_j = Depthofthejointregioninmm$
$b_j =$ Breadth of the joint region in mm

From the below figure 17, it is clearly observed that the joint distortion factor decreases quite significantly by increasing the % dosage of PET waste fiber in to the concrete mix. 1.00 % inclusion indicates best improved results among all and decrement of joint distortion is reduced by 20% with compare to normal concrete.

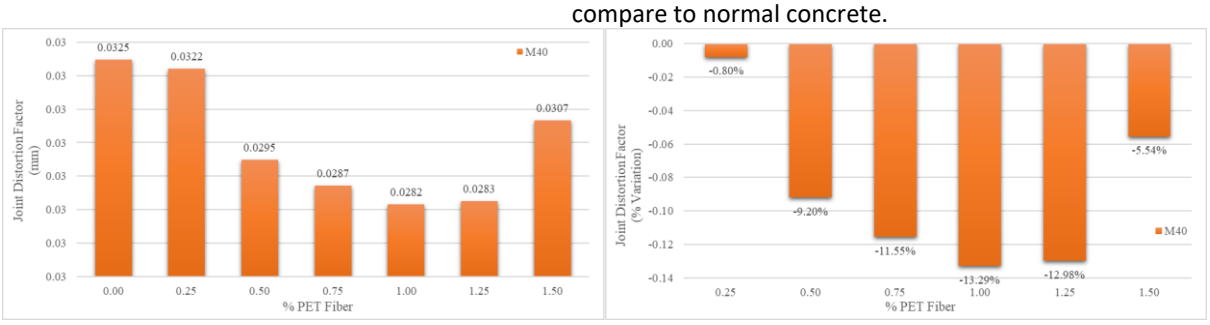

Fig. 17 Joint Distortion Factors for all specimens

Conclusion

This experiment is dealing with the new concept of developing sustainable concrete by incorporating post-consumer PET waste as a concrete material, it delivers dual benefit by reducing the natural material usage in concrete and major probability of utilizing waste product which improves the waste management.

The following are some of the major conclusive statements based on the research study;

- The compressive strength of the PET waste fiber concrete shows better results till 0.75 % inclusion of PET further addition of PET fiber indicates downfall of the concrete strength. Compressive strength of PET fiber concrete increases up to 6.10% with compare to conventional concrete.
- PET fiber concrete indicates incremental graph for the flexural strength till 1.00 % dosage of the waste fiber and the optimum increment value is 18.56 % higher than the conventional concrete.
- For the splitting tensile strength, it is observed that the strength values are kept increasing for all the specimen and its optimum increment reaches up to 14.00 % with compare to plain concrete.
- By adding PET waste fiber, the load carrying capacity of the concrete is increased. The optimum increment of the load carrying capacity touches up to 24.17 % for the 0.75 % specimen.
- For the beam-column junction, 0.75 % of PET fiber achieves 36.80 % additional energy dissipation compared to normal concrete.
- From the FEM analysis, it is indicated that the beam-column junction having waste fiber concrete, the ultimate stress, curvature ductility factor and shear resisting capacity are improving by 6.83 %, 19 % and 24 % respectively.

All the above-mentioned results indicate that the between 0.50 % to 1.00 % inclusion of PET waste fiber gives optimum values for the beam-column junction under the seismic condition. And also, by adding PET waste fiber can reduce the cost around 15 % with compared to conventional concrete junction under the seismic effect.

Conflicts of Interest

"The authordeclares that there is no conflict of interest regarding the publication of this paper."

Acknowledgments

Authors are obliged to Mr. Archal Shah, Founder of Composites Tomorrow, Vadodara for providing supply of all raw materials required and friendly support for the performance of experiments.

References

[1] Pacheco-Torgal F. Introduction to the use of recycled plastics in eco-efficient concrete. In: Use of Recycled Plastics in Eco-efficient Concrete. Elsevier; 2019. p. 1–8.

[2] Whinfield J, Dickson J. Improvements Relating to the Manufacture of Highly Polymeric Substances. UK Patent. 1941;578.

[3] Bhogayata A, Arora NK. Green concrete from the post-consumer plastic wastes: Indian scenario. 2011;437–40.

[4] Jain A. Fresh, strength, durability and microstructural properties of shredded waste plastic concrete. Iran. J Sci Technol Trans Civ Eng. 2019;43(1):455–65.

[5] Rahmani E, Dehestani M, Beygi MH, Allahyari H, Nikbin IM. On the mechanical properties of concrete containing waste PET particles, Constr. Constr Build Mater. 2013; 47:1302–8.

[6] Nirav M, Patel MN. Behavioral Changes in Strength of Concrete Reinforced by Waste Plastic

[7] Fibers. Information and Communication Technology for

[8]

[9] Competitive Strategies [Internet]. Vol. 191. Singapore: Springer; Available from: http://dx.doi.org/10.1007/978-981-16-0739-4_41

[10] Yang S, Yue X, Liu X, Tong Y. Properties of self-compacting lightweight concrete containing recycled plastic particles. Constr Build Mater [Internet]. 2015; 84:444–53. Available from: http://dx.doi.org/10.1016/j.conbuildmat.2015.03.038

[11] Foti D. Use of recycled waste pet bottles fibers for the reinforcement of concrete, Compos. Compos Struct. 2013; 96:396–404.

[12] Foti D. Preliminary analysis of concrete reinforced with waste bottles PET fibers, Constr. Constr Build Mater. 2011;25(4):1906–15.

[13] Nirav M, Patel DMN. Strength Performance of Concrete by using Polyethylene-Terephthalate Waste Fibers as Concrete Constitute. Design Engineering. 2021;141–56.

[14] Paul R, Melvin R. Increased joint hoop spacing in Type 2 seismic joints using fibre reinforced concrete. ACI Structural Journal. 1989;(2):168–72.

[15] Filatrault A, Ladicani K, Massicotte B. Seismic performance of code designed fibre reinforced concrete joints. ACI Structural Journal. 1994;91(5):564–71.

[16] Filiatrault A, Pineau S, Houde J. Seismic behaviour of steel fibre reinforced concrete interior beam-column joints. ACI Structural Journal. 1995;92(5):543–51.

[17] Thanukumari B, Perumal P. Behaviour of M60 Concrete Using Fibre Cocktail in Exterior Beam-Column Joint Under Reversed Cyclic Loading". Asian Journal of Civil Engineering (Building and Housing). 2010;11(2):265–75.

[18] Thanukumari B, Perumal P. An Experimental Study on the Behaviour of M20 Concrete with Cocktail Fibre in Exterior BeamColumn Joints Subjected to Reversed Cyclic Loading". IETECH Journal of Civil and Structures. 2009;2(2):65–070.

[19] Thanukumari B, Perumal P. Use of Fibre Cocktails to Increase the Seismic Performance of Beam-Column Joints". International Journal of Engineering Science and Technology. 2010;2(9):3997–4006.

[20] Thanukumari B, Perumal P. Role of Hybrid Fibres on the Ductility of Concrete in the Beam Column Joint Subjected to Seismic Loading". Journal of Structural Engineering.

[21] Dhabliya, D. (2022). Audit of Apache Spark Engineering in Data Science and Examination of Its Functioning Component and Restrictions and Advantages. INTERNATIONAL JOURNAL OF MANAGEMENT AND ENGINEERING RESEARCH, 2(1), 01–04.

[22] Thanukumari B, Perumal P. Seismic Behaviour of Fibre Reinforced Concrete by Using Various Types of Fibres". In: Proceedings of the National Conference on the Recent Development in Concrete Technology. Coimbatore; 2006. p. 445–59.

[23] Rabanal, N., & Dhabliya, D. (2022). Designing Architecture of Embedded System Design using HDL Method. Acta Energetica, (02), 52–58.

[24] Thanukumari B, Perumal P. Behaviour of High-Performance Fibre Reinforced Exterior Beam Column Joint Under Cyclic Loading". In: Proceedings of the International Conference on Innovative and Smart Structural Systems for Sustainable Habitat. 2008. p. 59–60.

[25] Thanukumari B, Perumal P. Behaviour of Fibre Reinforced Exterior Beam Column Joint Subjected to Cyclic Load". In: Proceedings of the National Conference on Advances in Construction Materials, Methods and Management (AC3M-'09) at Chaitanya Bharathi Institute of Technology, Hydrabad. 2009. p. 429–36.

[26] Thanukumari B, Perumal P. Cyclic Load Behaviour of M20 Concrete in Exterior Beam column Joint Using Cocktail Fibre". In: Proceedings of the National Conference on the Advances in the Steel Concrete Composite Structures (ASCCS-'09. Coimbatore; 2009. p. E30–4.

[27] Juneja, V., Singh, S., Jain, V., Pandey, K. K., Dhabliya, D., Gupta, A., & Pandey, D. (2023). Optimization-Based Data Science for an IoT Service Applicable in Smart Cities. In Handbook of Research on Data-Driven Mathematical Modeling in Smart Cities (pp. 300–321). IGI Global.

[28] Bureau of Indian Standards. IS 456: Plain and Reinforced Concrete - Code of Practice [Internet]. https://archive.org/details/gov.in.is.456.2000. Available from: Public.Resource.Org

[29] Bureau of Indian Standards. IS 1893-1 (2002): Criteria for Earthquake Resistant Design of Structures, Part 1: General Provisions and Buildings [Internet]. https://archive.org/details/gov.in.is.1893.1.2002. Available from: Public.Resource.Org

[30] Ganganagoudar A, Mondal TG, Suriya Prakash S. Analytical and finite element studies on behavior of FRP strengthened RC beams under torsion. Compos Struct [Internet]. 2016;153:876–85. Available from: http://dx.doi.org/10.1016/j.compstruct.2016.07.014

[31] Belarbi A, Hsu TTC. Constitutive laws of concrete in tension and reinforcing bars stiffened by concrete. ACI Struct J. 1994;91(4):465–74.

[32] Murty CVR, Durgesh C, Bajpai KK, Jain K. Effectiveness of Reinforcement Details in Exterior Reinforced Concrete Beam-Column Joints for Earthquake Resistance". ACI Structural Journal. 2003;100(2):149–56.

[33] Ganesan N, Indira PV. Latex modified SFRC beam-column joints subjected to cyclic loading". The Indian Concrete Journal. 2000;416–20.